



# Multistability in an age-structured model of hematopoiesis: Cyclical neutropenia

Jinzhi Lei<sup>a,\*</sup>, Michael C. Mackey<sup>b</sup>

<sup>a</sup> Zhou Pei-Yuan Center for Applied Mathematics, Tsinghua University, Beijing, China

<sup>b</sup> Departments of Physiology, Physics, and Mathematics, Centre for Nonlinear Dynamics, McGill University, Montreal, QC, Canada

## ARTICLE INFO

### Article history:

Received 1 April 2010

Received in revised form

21 September 2010

Accepted 13 November 2010

Available online 19 November 2010

### Keywords:

Hematopoietic disease

Dynamical disease

Delay differential equation

Bifurcation

## ABSTRACT

Cyclical neutropenia (CN) is a rare hematopoietic disorder in which the patient's neutrophil level drops to extremely low levels for a few days approximately every three weeks. CN is effectively treated with granulocyte colony stimulating factor (G-CSF), which is known to interfere with apoptosis in neutrophil precursors and to consequently increase the circulating neutrophil level. However, G-CSF treatment usually fails to eliminate the oscillation. In this study, we establish an age-structured model of hematopoiesis, which reduces to a set of four delay differential equations with specific forms of initial functions. We numerically investigate the possible stable solutions of the model equations with respect to changes in the parameters as well as the initial conditions. The results show that the hematopoietic system possesses multistability for parameters typical of the normal healthy state. From our numerical results, decreasing the proliferation rate of neutrophil precursors or increasing the stem cell death rate are two possible mechanisms to induce cyclical neutropenia, and the periods of the resulting oscillations are independent of the changing parameters. We also discuss the dependence of the model solution on the initial condition at normal parameter values corresponding to a healthy state. Using insight from our results we design a hybrid treatment method that is able to abolish the oscillations in CN.

© 2010 Elsevier Ltd. All rights reserved.

## 1. Introduction

The hematopoietic regulatory system is a dynamical system with negative feedback control of all circulating cellular blood components. In a healthy adult person, approximately  $10^{11}$ – $10^{12}$  new blood cells are produced daily in order to maintain the steady state levels in the peripheral circulation. All blood cells are derived from a common origin in the bone marrow, the hematopoietic stem cells (HSCs). These stem cells differentiate and proliferate, giving rise to the three major cell lines: the leukocytes (white blood cells), erythrocytes (red blood cells), and platelets. The three peripheral regulatory loops are of a negative feedback nature. They are mediated by a variety of cytokines including granulocyte colony stimulating factor (G-CSF) (Price et al., 1996), which regulates neutrophil numbers, erythropoietin (EPO) (Adamson, 1999), which mediates the regulation of erythrocyte production, and thrombopoietin (TPO) (Ratajczak et al., 1997; Tanimukai et al., 1997), which regulates production of platelets and other cell lineages. These cytokines are synthesized and released by cells of the hematopoietic system. Despite the fact that the broad outlines of the

regulation process are clear, the detailed dynamics of how the numbers of circulating cells of each type are regulated remain somewhat obscure and have been attracting widespread interest from different contexts (Collijn and Mackey, 2005a,b; Dingli et al., 2007; Foo et al., 2009; Foley and Mackey, 2009; Lei and Mackey, 2007; Mahaffy et al., 1998; Marciniak-Czochra et al., 2009; Ostby et al., 2004; Roeder et al., 2009; Rubinow and Lebowitz, 1975). Deregulation of hematopoiesis can result in a number of hematological diseases with significant oscillations in one or more of the circulating cells (Haurie et al., 1998; Foley and Mackey, 2009). Examples of these diseases include cyclical neutropenia (CN) (Colijn and Mackey, 2005b; Haurie et al., 1998, 1999a; von Schulthess and Mazer, 1982), periodic chronic myelogenous leukemia (PCML) (Colijn and Mackey, 2005a; Fortin and Mackey, 1999; Pujo-Menjouet and Mackey, 2004), cyclical thrombocytopenia (CT) (Apostu and Mackey, 2008; Pavord et al., 1996; Santillan et al., 2000), and periodic auto-immune hemolytic anemia (AIHA) (Mackey, 1979; Milton and Mackey, 1989). Of particular interest in this paper is cyclical neutropenia.

Neutrophils are a class of white blood cells and comprise approximately 60% of the blood cells. These cells are critically important for the immune response and migrate from the blood to tissue during an infection to destroy pathogens. Cyclical neutropenia is a type of severe chronic neutropenia with recurrent low absolute neutrophil counts in the blood and CN patients therefore

\* Corresponding author.

E-mail addresses: [jzlei@mail.tsinghua.edu.cn](mailto:jzlei@mail.tsinghua.edu.cn) (J. Lei), [mackey@cnd.mcgill.ca](mailto:mackey@cnd.mcgill.ca) (M.C. Mackey).

have recurrent infections as a clinical symptom. Patients with CN are characterized by oscillations in the circulating neutrophil count. The neutrophil count falls from normal to barely detectable levels with a period of about 19–21 days (Guerry et al., 1973; Dale and Hammond, 1988; Haurie et al., 1999b), although longer periods have been observed (Haurie et al., 1999b). CN is also found in an animal model, the grey collie (Lund et al., 1967). The canine disorder closely resembles human CN with the exception of the period that ranges from 11 to 15 days (Haurie et al., 1999a). In both humans with CN and the grey collie, there is not only a periodic decrease in the circulating neutrophil levels, but also a corresponding oscillation of platelets, and occasionally the reticulocytes and lymphocytes. Often (but not always), the period of the oscillation in these other cell lines is the same as the period in the neutrophils (Haurie et al., 1998, 1999a,b).

Cyclical neutropenia in humans is often treated using G-CSF (Hammond et al., 1989), which is known to interfere with neutrophil precursor apoptosis (Koury, 1992; Park, 1996; Migliaccio et al., 1990; Williams and Smith, 1993). Administering G-CSF to CN patients usually results in an increased amplitude and decreased period of the oscillations. In some isolated cases, G-CSF abolished the oscillations (Haurie et al., 1999b; Hammond et al., 1989). The reason for the diverse responses to G-CSF treatment remains unclear.

In Bernard et al. (2003), a two-compartment model of HSCs and the circulating neutrophils was used to study the origins of oscillations in CN and to mimic the effect of G-CSF treatment. In Foley and Mackey (2006), the same two-compartment model was used to study the effects of G-CSF treatment with different protocols. It was shown that, depending on the starting time of G-CSF administration, the neutrophil count could either be stabilized or show large amplitude oscillations. Similar results were also noted in Colijn et al. (2007) in a more comprehensive four-compartment model that was developed earlier (Colijn and Mackey, 2005a,b). All these results suggest the possible co-existence of both a stable steady state and oscillatory neutrophil counts (bistability) in the hematopoietic regulatory system. The bistability was described in a two-compartment model, but the parameters were away from the typical normal values (Bernard et al., 2003).

Numerical simulations also found multiple oscillatory solutions in both two- and four-compartment models (Bernard et al., 2003; Colijn et al., 2007). However, the range of the system parameters over which this bistability exists was not clear. In particular, it is not clear whether the system would have bistability in the typical healthy state, or in a state of post G-CSF treatment, and how the oscillatory state in G-CSF treatment could be avoided.

In this paper, we numerically study the multistability in hematopoietic regulation. This is done by investigating the possible stable solutions of the system corresponding to different system parameters and initial conditions. We will first introduce in Section 2 an age-structured model of hematopoiesis, which is described by a set of delay differential equation with particular forms for the initial functions. In Section 3, we will discuss the bifurcation and multistability of the model, and the effect of initial conditions. At the end of this section, we propose a hybrid method that combines G-CSF administration and blood transfusion/hemospasia as a possible treatment for CN. Simulations show that this hybrid method is able to abolish the oscillation. The paper concludes with a discussion in Section 4.

## 2. Model and method

### 2.1. Model formulation

In previous work the dynamics of the hematopoietic system has been modeled by a set of nonlinear delay differential equations (Colijn and Mackey, 2005a,b), which was obtained from the age-structured models of the stem cell population (Mackey, 1978), leukocytes (Hearn et al., 1998; Haurie et al., 2000; Bernard et al., 2003), erythrocytes (Mackey, 1979; Bélair et al., 1995; Mahaffy et al., 1998) and platelets (Bélair and Mackey, 1987; Santillan et al., 2000). We refer this model in the present study.

The model under study is illustrated in Fig. 1. There are four compartments, including the stem cells and three differentiated cell lines.

Stem cells are classified as resting-phase ( $G_0$ ) cells (population  $Q(t)$ , cells/kg) or proliferating-phase (population  $s(t,a)$ , cells/kg)

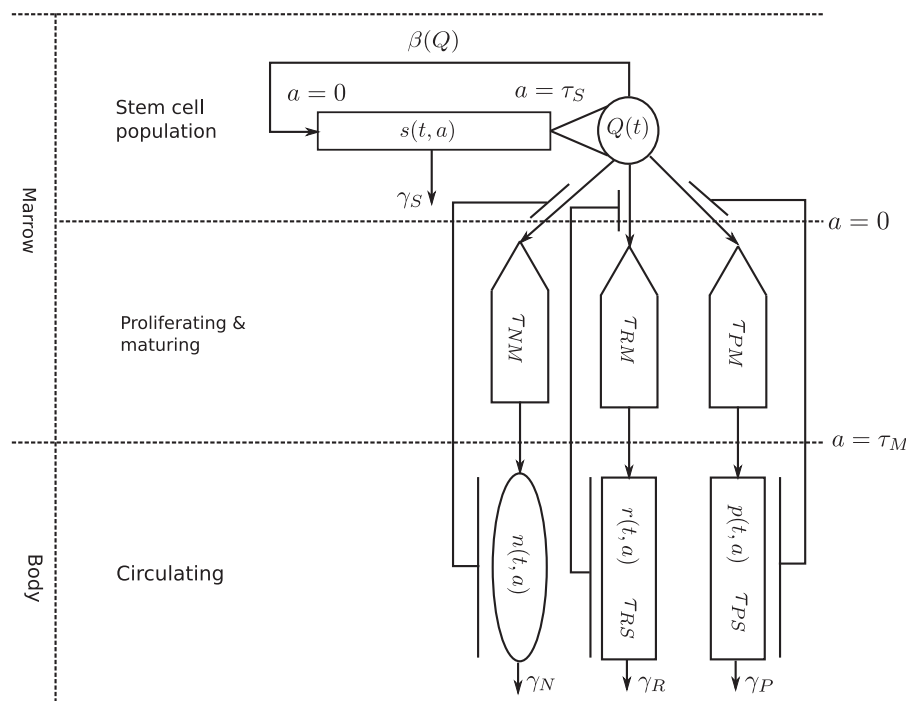


Fig. 1. A cartoon representation of the age-structured model. See text for details and notation.

(Mackey, 1978). The resting-phase cells can either re-enter the proliferative phase at a rate  $\beta(Q)$  ( $\text{day}^{-1}$ ) that involves a negative feedback, or differentiate into any of the three cell lines, leukocytes (population  $n(t,a)$ , cells/kg), erythrocytes (population  $r(t,a)$ , cells/kg), or platelets (population  $p(t,a)$ , cells/kg), at rates  $\kappa_N$  ( $\text{day}^{-1}$ ),  $\kappa_R$  ( $\text{day}^{-1}$ ), or  $\kappa_P$  ( $\text{day}^{-1}$ ), respectively. An age-structured quantity  $s(t,a)$  is used to represent the population of proliferating stem cells, with the age  $a=0$  for their time of entry into the proliferative state. Moreover, the proliferating stem cells are assumed to undergo mitosis at a fixed time  $\tau_S$  after entry into the proliferating compartment, and to be lost randomly at a rate  $\gamma_S$  ( $\text{day}^{-1}$ ) during the proliferating phase (Mackey, 1996). Each normal cell generates two resting-phase cells at the end of mitosis.

Age-structured models are used for the dynamics of leukocytes, erythrocytes, and platelets, with age  $a=0$  for the time point of differentiating from stem cells. All the differentiation rates  $\kappa_N(N)$ ,  $\kappa_R(R)$ , and  $\kappa_P(P)$  involve negative feedback loops, with the rates depending on the population of the corresponding circulating cells  $N(t)$ ,  $R(t)$ , and  $P(t)$ , respectively (Colijn and Mackey, 2005a). There are two stages for each of the circulating cell lines after the differentiation, first the amplification/maturation of precursor cells in the bone marrow, and next circulation of mature cells throughout the body. In the stage of amplification/maturation, the precursor cells undergo many stages of cell division and randomly die in a period of  $\tau_{NM}$  (days) for leukocytes,  $\tau_{RM}$  (days) for erythrocytes, and  $\tau_{PM}$  (days) for platelets, respectively. The proliferation rates of the precursor cells are represented by  $\eta_N$  for leukocytes,  $\eta_R$  for erythrocytes, and  $\eta_P$  for platelets, and are positive and assumed to be constants. Thus, increasing the apoptosis rate of precursor cells can result in a decrease of the proliferation rates. Circulating cells are lost at rates  $\gamma_N$ ,  $\gamma_R$ , and  $\gamma_P$ , respectively. In addition, the circulating erythrocytes and platelets are actively destroyed at a fixed time  $\tau_{RS}$  and  $\tau_{PS}$ , respectively, from their time of entering the circulating compartment (Mahaffy et al., 1998; Bélair and Mackey, 1987).

Let

$$\begin{aligned} N(t) &= \int_{\tau_{NM}}^{+\infty} n(t,a) da \\ R(t) &= \int_{\tau_{RM}}^{\tau_{Rsum}} r(t,a) da \\ P(t) &= \int_{\tau_{PM}}^{\tau_{Psum}} p(t,a) da, \end{aligned} \quad (1)$$

which are the populations of circulating cells. Hereinafter we set  $\tau_{Rsum} = \tau_{RM} + \tau_{RS}$ ,  $\tau_{Psum} = \tau_{PM} + \tau_{PS}$ . Also let

$$\kappa(t) = \kappa_N(N(t)) + \kappa_R(R(t)) + \kappa_P(P(t)) \quad (2)$$

denote the total HSC differentiation rate of stem cells at time  $t$ . The model is then described by the following partial differential equations

$$\begin{aligned} \nabla s(t,a) &= -\gamma_S s(t,a) \quad (t > 0, 0 \leq a \leq \tau_S) \\ \frac{dQ}{dt} &= 2s(t,\tau_S) - (\beta(Q) + \kappa(t))Q \quad (t > 0) \\ \nabla n(t,a) &= \begin{cases} \eta_N n(t,a) & (t > 0, 0 \leq a \leq \tau_{NM}) \\ -\gamma_N n(t,a) & (t > 0, a \geq \tau_{NM}) \end{cases} \\ \nabla r(t,a) &= \begin{cases} \eta_R r(t,a) & (t > 0, 0 \leq a \leq \tau_{RM}) \\ -\gamma_R r(t,a) & (t > 0, \tau_{RM} \leq a \leq \tau_{Rsum}) \end{cases} \\ \nabla p(t,a) &= \begin{cases} \eta_P p(t,a) & (t > 0, 0 \leq a \leq \tau_{PM}) \\ -\gamma_P p(t,a) & (t > 0, \tau_{PM} \leq a \leq \tau_{Psum}) \end{cases} \end{aligned} \quad (3)$$

where  $\nabla = \partial/\partial t + \partial/\partial a$ .

The negative feedback functions are represented by Hill functions (Colijn and Mackey, 2005a)

$$\kappa_N(N) = f_0 \frac{\theta_1^{s_1}}{\theta_1^{s_1} + N^{s_1}}, \quad \beta(Q) = k_0 \frac{\theta_2^{s_2}}{\theta_2^{s_2} + Q^{s_2}}, \quad (4)$$

$$\kappa_R(R) = \frac{\bar{\kappa}_R}{1 + K_R R^{s_3}}, \quad \kappa_P(P) = \frac{\bar{\kappa}_P}{1 + K_P P^{s_4}}. \quad (5)$$

The boundary conditions at  $a=0$  are given by

$$\begin{aligned} s(t,0) &= \beta(Q(t))Q(t), \\ n(t,0) &= \kappa_N(N(t))Q(t), \\ r(t,0) &= \kappa_R(R(t))Q(t), \\ p(t,0) &= \kappa_P(P(t))Q(t), \end{aligned} \quad (t \geq 0) \quad (6)$$

according to the negative feedback loops. The initial conditions are  $s(0,a) = g_S(a)$ , ( $0 \leq a \leq \tau_S$ )

$$\begin{aligned} Q(0) &= Q_0 \\ n(0,a) &= g_N(a), \quad (0 \leq a \leq +\infty) \\ r(0,a) &= g_R(a), \quad (0 \leq a \leq \tau_{Rsum}) \\ p(0,a) &= g_P(a), \quad (0 \leq a \leq \tau_{Psum}) \end{aligned} \quad (7)$$

Eqs. (1)–(7) define the initial-boundary value problem for the age-structured model of hematopoietic regulation.

When  $t > \tau_{max} = \max\{\tau_S, \tau_{NM}, \tau_{Rsum}, \tau_{Psum}\}$ , we integrate Eq. (3) by the method of characteristics to obtain the following model of delay differential equations that has been studied in Colijn and Mackey (2005a,b, 2007):

$$\begin{aligned} \frac{dQ}{dt} &= -(\beta(Q) + \kappa_N(N) + \kappa_R(R) + \kappa_P(P))Q + 2e^{-\gamma_S \tau_S} \beta(Q_{\tau_S})Q_{\tau_S}, \\ \frac{dN}{dt} &= -\gamma_N N + e^{\eta_N \tau_{NM}} \kappa_N(N_{\tau_{NM}})Q_{\tau_{NM}}, \\ \frac{dR}{dt} &= -\gamma_R R + e^{\eta_R \tau_{RM}} \{\kappa_R(R_{\tau_{RM}})Q_{\tau_{RM}} - e^{-\gamma_R \tau_{RS}} \kappa_R(R_{\tau_{Rsum}})Q_{\tau_{Rsum}}\}, \\ \frac{dP}{dt} &= -\gamma_P P + e^{\eta_P \tau_{PM}} \{\kappa_P(P_{\tau_{PM}})Q_{\tau_{PM}} - e^{-\gamma_P \tau_{PS}} \kappa_P(P_{\tau_{Psum}})Q_{\tau_{Psum}}\}. \end{aligned} \quad (8)$$

Here, the subscripts on the dependent variables indicate delayed arguments, i.e.,  $Q_{\tau_S} = Q(t - \tau_S)$ .

When  $t \leq \tau_{max}$ , the initial conditions (7) have to be taken into account. Note that  $\tau_{RM} < \tau_{RS}$  in hematopoietic regulation (Colijn and Mackey, 2005a). In Appendix A, we obtain the following model equations starting from  $t \geq 0$  by applying the method of characteristics to (3)

$$\begin{aligned} \frac{dQ}{dt} &= -(\beta(Q) + \kappa_N(N) + \kappa_R(R) + \kappa_P(P))Q + F_Q(t) \\ \frac{dN}{dt} &= -\gamma_N N + F_N(t) \\ \frac{dR}{dt} &= -\gamma_R R + F_R(t) \\ \frac{dP}{dt} &= -\gamma_P P + F_P(t) \end{aligned} \quad (9)$$

where  $F_Q(t)$ ,  $F_N(t)$ ,  $F_R(t)$  and  $F_P(t)$  are piecewise continuous functions given in Table 1.

Let  $(Q(0), N(0), R(0), P(0)) = (Q_0, N_0, R_0, P_0)$  be the initial condition of (9). In Eq. (3), compatibility between the initial and boundary conditions at  $(0,0)$  requires the following equalities

$$(g_S(0), g_N(0), g_R(0), g_P(0)) = (\beta(Q_0)Q_0, \kappa_N(N_0)Q_0, \kappa_R(R_0)Q_0, \kappa_P(P_0)Q_0), \quad (10)$$

**Table 1**  
Definition of the functions  $F_Q(t)$ ,  $F_N(t)$ ,  $F_R(t)$  and  $F_P(t)$ .

The functions  $F_Q(t)$ ,  $F_N(t)$  and  $F_R(t)$  are

$$F_Q(t) = \begin{cases} 2g_S(\tau_S - t)e^{-\gamma_S t}, & (0 \leq t \leq \tau_S) \\ 2e^{-\gamma_S \tau_S} \beta(Q_{\tau_S})Q_{\tau_S}, & (t > \tau_S) \end{cases}$$

$$F_N(t) = \begin{cases} g_N(\tau_{NM} - t)e^{\eta_N t}, & (0 \leq t \leq \tau_{NM}) \\ e^{\eta_N \tau_{NM}} \kappa_N(N_{\tau_{NM}})Q_{\tau_{NM}}, & (t > \tau_{NM}) \end{cases}$$

$$F_R(t) = \begin{cases} g_R(\tau_{RM} - t)e^{\eta_R t} - g_R(\tau_{Rsum} - t)e^{-\gamma_R t}, & (0 \leq t \leq \tau_{RM}) \\ e^{\eta_R \tau_{RM}} \kappa_R(R_{\tau_{RM}})Q_{\tau_{RM}} - g_R(\tau_{Rsum} - t)e^{-\gamma_R t}, & (\tau_{RM} < t \leq \tau_{RS}) \\ e^{\eta_R \tau_{RM}} \kappa_R(R_{\tau_{RM}})Q_{\tau_{RM}} - g_R(\tau_{Rsum} - t)e^{-\gamma_R \tau_{RS} + \eta_R(t - \tau_{RS})}, & (\tau_{RS} < t \leq \tau_{Rsum}) \\ e^{\eta_R \tau_{RM}} \{ \kappa_R(R_{\tau_{RM}})Q_{\tau_{RM}} - e^{-\gamma_R \tau_{RS}} \kappa_R(R_{\tau_{Rsum}})Q_{\tau_{Rsum}} \}, & (t > \tau_{Rsum}) \end{cases}$$

If  $\tau_{PM} \leq \tau_{PS}$ ,

$$F_P(t) = \begin{cases} g_P(\tau_{PM} - t)e^{\eta_P t} - g_P(\tau_{Psum} - t)e^{-\gamma_P t}, & (0 \leq t \leq \tau_{PM}) \\ e^{\eta_P \tau_{PM}} \kappa_P(P_{\tau_{PM}})Q_{\tau_{PM}} - g_P(\tau_{Psum} - t)e^{-\gamma_P t}, & (\tau_{PM} < t \leq \tau_{PS}) \\ e^{\eta_P \tau_{PM}} \kappa_P(P_{\tau_{PM}})Q_{\tau_{PM}} - g_P(\tau_{Psum} - t)e^{-\gamma_P \tau_{PS} + \eta_P(t - \tau_{PS})}, & (\tau_{PS} < t \leq \tau_{Psum}) \\ e^{\eta_P \tau_{PM}} \{ \kappa_P(P_{\tau_{PM}})Q_{\tau_{PM}} - e^{-\gamma_P \tau_{PS}} \kappa_P(P_{\tau_{Psum}})Q_{\tau_{Psum}} \}, & (t > \tau_{Psum}) \end{cases}$$

and if  $\tau_{PS} < \tau_{PM}$ ,

$$F_P(t) = \begin{cases} g_P(\tau_{PM} - t)e^{\eta_P t} - g_P(\tau_{Psum} - t)e^{-\gamma_P t}, & (0 \leq t \leq \tau_{PS}) \\ g_P(\tau_{PM} - t)e^{\eta_P t} - g_P(\tau_{Psum} - t)e^{-\gamma_P \tau_{PS} + \eta_P(t - \tau_{PS})}, & (\tau_{PS} < t \leq \tau_{PM}) \\ e^{\eta_P \tau_{PM}} \kappa_P(P_{\tau_{PM}})Q_{\tau_{PM}} - g_P(\tau_{Psum} - t)e^{-\gamma_P \tau_{PS} + \eta_P(t - \tau_{PS})}, & (\tau_{PM} < t \leq \tau_{Psum}) \\ e^{\eta_P \tau_{PM}} \{ \kappa_P(P_{\tau_{PM}})Q_{\tau_{PM}} - e^{-\gamma_P \tau_{PS}} \kappa_P(P_{\tau_{Psum}})Q_{\tau_{Psum}} \}, & (t > \tau_{Psum}) \end{cases}$$

and

$$(\beta'(Q_0)Q_0 + \beta(Q_0))Q'(0) + g_S'(0) = -\gamma_S g_S(0),$$

$$Q'(0) = 2g_S(\tau_S) - (\beta(Q_0) + \kappa(0))Q_0,$$

$$\kappa'_N(N_0)N'(0)Q_0 + \kappa_N(N_0)Q'(0) + g'_N(0) = \eta_N g_N(0), \tag{11}$$

$$\kappa'_R(R_0)R'(0)Q_0 + \kappa_R(R_0)Q'(0) + g'_R(0) = \eta_R g_R(0),$$

$$\kappa'_P(P_0)P'(0)Q_0 + \kappa_P(P_0)Q'(0) + g'_P(0) = \eta_P g_P(0),$$

where  $(N_0, R_0, P_0)$  are associated with the initial population distributions through

$$N_0 = \int_{\tau_{NM}}^{+\infty} g_N(a) da, \quad R_0 = \int_{\tau_{RM}}^{\tau_{Rsum}} g_R(a) da, \quad P_0 = \int_{\tau_{PM}}^{\tau_{Psum}} g_P(a) da, \tag{12}$$

and  $Q'(0), N'(0), R'(0), P'(0)$  are given by (9) at  $t=0$ .

Eqs. (9)–(12) give a model of hematopoietic regulation from the original age-structured model (3)–(7). Initial conditions of the delay differential Eq. (8) are given explicitly through the initial populations  $g_i(a)$ , ( $i=S, N, R, P$ ) with the restrictions (10)–(12) and the Eq. (9) with  $0 \leq t \leq \tau_{max}$ .

In Colijn and Mackey (2007), bifurcations, bistability, and the effect of initial functions in the delay differential equation model were studied by solving the equations numerically with predefined initial functions on  $-\tau_{max} \leq t \leq 0$  (corresponding to the initial functions in the present model with  $0 < t < \tau_{max}$ ). Nevertheless, solutions obtained in this way, with positive initial conditions, can be negative at some time  $t > 0$  and therefore biologically not acceptable. This indicates that there is no equivalent between a delay model and an age-structured model when initial conditions are not taken into considerations. In the present model, if the initial populations  $g_i(a)$  satisfy (10)–(12), we can prove that any solution of Eq. (9) with positive initial conditions  $(Q_0, N_0, R_0, P_0)$  is positive for all  $t > 0$ <sup>1</sup>.

## 2.2. Method

This study focuses on the stable oscillatory solutions with dynamical properties similar to those in patients with CN. In the

<sup>1</sup> For example, see Appendix A for a brief discussion. A detailed proof will be given elsewhere.

**Table 2**  
Normal steady state parameters.

Sources: 1 = Bernard et al. (2003), 2 = Abkowitz et al. (1988), 3 = Beutler et al. (1995), 4 = Deubelbeiss et al. (1975), 5 = Haurie et al. (2000), 6 = Mahaffy et al. (1998), 7 = Novak and Necas (1994), 8 = Santillan et al. (2000).

Parameter name	Value used	Unit	Sources
<i>Stem cell compartment</i>			
$Q_*$	1.1	$\times 10^6$ cells/kg	1
$\gamma_S$	0.07	day <sup>-1</sup>	1
$\tau_S$	2.8	days	1,2
$k_0$	8.0	day <sup>-1</sup>	1
$\theta_2$	0.3	$\times 10^6$ cells/kg	1
$s_2$	4	(none)	1
<i>Neutrophil compartment</i>			
$N_*$	6.9	$\times 10^8$ cells/kg	2,3
$\gamma_N$	2.4	day <sup>-1</sup>	1,4,5
$\tau_{NM}$	3.5	days	1
$\eta_N$	3.208	day <sup>-1</sup>	1,3
$f_0$	0.40	day <sup>-1</sup>	(calculated)
$\theta_1$	0.36	$\times 10^8$ cells/kg	1
$s_1$	1	(none)	1
<i>Erythrocyte compartment</i>			
$R_*$	3.5	$\times 10^{11}$ cells/kg	6
$\gamma_R$	0.001	day <sup>-1</sup>	6
$\tau_{RM}$	6	days	6
$\tau_{Rsum}$	120	days	6
$\eta_R$	1.8222	day <sup>-1</sup>	3,7
$\bar{K}_r$	1.17	day <sup>-1</sup>	(calculated)
$K_r$	0.0382	$(\times 10^{11} \text{ cells/kg})^{-s_3}$	6
$s_3$	6.96	(none)	6
<i>Platelet compartment</i>			
$P_*$	2.94	$\times 10^{10}$ cells/kg	8
$\gamma_P$	0.15	day <sup>-1</sup>	8
$\tau_{PM}$	7	days	8
$\tau_{PS}$	9.5	days	8
$\eta_P$	1.46	day <sup>-1</sup>	3
$\bar{K}_p$	1.17	day <sup>-1</sup>	(calculated)
$K_p$	11.66	$(\times 10^{10} \text{ cells/kg})^{-s_4}$	8
$s_4$	1.29	(none)	8

current study, we solve the model equations numerically to seek possible stable solutions corresponding to given parameters. The solutions could be considered as biologically possible states when the system parameters are changed for some reason.

From previous studies (Bernard et al., 2003; Colijn and Mackey, 2005b), the possible mechanisms leading to the oscillation in CN include a decrease of the proliferation rate of neutrophil precursor cells, and an increase of the apoptosis rate of stem cells. Accordingly, the proliferation rate of the neutrophil precursor cells  $\eta_N$  and the stem cell death rate  $\gamma_S$  are two parameters of interest in the current study. In addition, G-CSF treatment is known to decrease the apoptosis in neutrophil precursors, which results in an increase of  $\eta_N$ , and an increase of the stem cell differentiation rate  $\kappa_N$  by increasing  $\theta_1$  (Bernard et al., 2003; Colijn et al., 2007). The parameter  $\theta_1$  is proportional to the production of G-CSF (Bernard et al., 2003). Therefore, We are also interested in the parameter  $\theta_1$ . In the simulations, we change each of these parameters, and hold the other parameters at their default values as given in Table 2, which are estimated to correspond to the healthy state (Colijn and Mackey, 2005a).

From Colijn and Mackey (2005a), in the case of a healthy state, the Eq. (9) possesses a positive steady state (when  $t > \tau_{max}$ ), denoted by  $(Q_*, N_*, R_*, P_*)$ . In our simulation, for each set of parameters, we solve the model equations numerically to obtain 20 independent sample solutions, each with randomly selected initial value at  $t=0$ . The initial values  $(Q_0, N_0, R_0, P_0)$  are taken randomly from the range

$$0.1 < Q_0/Q_*, N_0/N_*, R_0/R_*, P_0/P_* < 10.$$

The initial populations  $g_i$ , ( $i=S,N,R,P$ ) are defined according to the initial values and the conditions (10)–(12) (refer to Appendix B for details). Each solution is solved by Euler’s method (with time step  $dt = 0.002$ ) up to  $t = 1800$  days, such that it reaches a stable state (either oscillatory or steady state), and the resulting data from the last 600 days are used for further analysis as detailed below.

To distinguish oscillatory solutions from constant solutions in the simulation, we investigate the upper and lower bounds of the stem cell count  $Q(t)$  in the last 600 days of the simulation ( $1200 < t < 1800$  (days)), denoted by  $Q_{\max}$  and  $Q_{\min}$ , respectively. Therefore, a solution approaches the steady state if  $Q_{\max} \approx Q_{\min}$ , and approaches an oscillatory solution between  $Q_{\max}$  and  $Q_{\min}$  if  $Q_{\max} \gg Q_{\min}$ . For oscillatory solutions, we calculate the period by applying Lomb periodogram analysis to the neutrophil population  $N(t)$  in the last 600 days (Lomb, 1976), in accordance with the way one determines the periods from observed data (Haurie et al., 1999a,b).

Patients with CN have neutrophil levels lower than  $0.5 \times 10^9/L$ , about 1/10 of the normal level, for 3–5 days for every three weeks (Haurie et al., 1999b; Gill et al., 2000). To test this feature for each oscillatory solution quantitatively, we define the “severity index” of a solution as the average fraction of days, in the last 600 days in the simulation, such that the neutrophil count is less than  $0.1 \times N_*$ . A larger value of the severity index means a more severe manifestation of the disease in a given patient. In the case of a CN patient, the index takes a value of about  $4/20 = 0.2$ .

### 3. Results

#### 3.1. Bifurcation diagram and multistability

Fig. 2 shows the simulation result when either of the parameters,  $\gamma_S$ ,  $\eta_N$ , or  $\theta_1$  is changed.

Figs. 2 a–c show  $Q_{\max}$  and  $Q_{\min}$  of the solutions, which depend on the system parameters and initial conditions. Each solution gives two points,  $Q_{\max}$  and  $Q_{\min}$ , in each panel. The solutions converging to a stable steady state are indicated by the superposition of  $Q_{\max}$  and  $Q_{\min}$ , while the oscillatory solutions are characterized by the separating of  $Q_{\max}$  and  $Q_{\min}$ . The results show clear evidence for multistability over a wide range of parameter values, including typical parameter values for healthy states. In this multistable region, the system dynamics for the same parameter values can converge to either a stable steady state or an oscillatory state, depending on the initial conditions.

From Fig. 2a, when the neutrophil precursor proliferation rate  $\eta_N$  decreases from the default value, there is a critical point ( $\eta_N = 3.10$ ) at which the steady state becomes unstable. Nevertheless, the oscillatory state remains stable across this critical point. Similar results are also seen in the diagram with respect to the stem cell death rate  $\gamma_S$  and the parameter  $\theta_1$  (Figs. 2 b–c). Increasing either  $\gamma_S$  or  $\theta_1$  is able to destabilize the steady state, while the oscillatory state remains stable. Here, the critical values are  $\gamma_S = 0.082$  or  $\theta_1 = 0.51$ ,

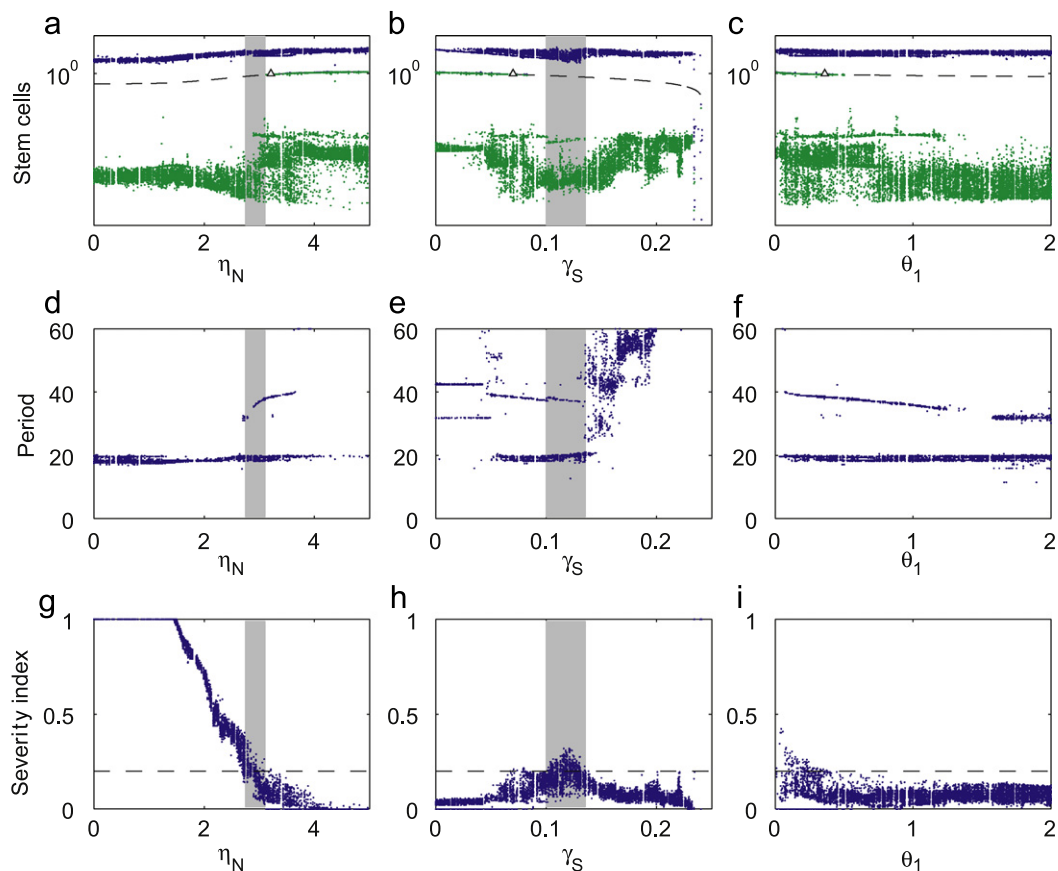


**Fig. 2.** The bifurcation diagrams. (a)–(c) The maximum (blue circle) and minimum (green plus) values of stem cell counts  $Q(t)$  (in units of  $10^6$  cells/kg) for each solution in the time interval  $1200 < t < 1800$  (days), with given system parameters as shown by the X-axis. Stable steady-states are shown by the superposition of the maximum and minimum values. Dashed lines show the stem cell counts for steady state solutions. Triangles show the points for default values as in Table 2. (d)–(f) The periods (in days) of neutrophils in the oscillatory solutions, obtained by Lomb periodogram analysis with significance level 0.01. (g)–(i) The severity index (refer the text for the definition) of the oscillatory solutions. Dashed lines show a severity index of 0.20. Shadows show the parameter regions in which there are oscillatory solutions with a period of about 20 days and severity index of about 0.20, in accordance with observed data from CN patients. (For interpretation of the references to colour in this figure legend, the reader is referred to the web version of this article.)

respectively. Stability of the oscillatory state is indicative of the persistence of CN as is observed clinically in G-CSF treatment. We shall discuss this later through the effect of initial conditions. In Fig. 2(b), we note that when  $\gamma_S$  is large enough ( $\gamma_S > 0.247$ ), the oscillatory solutions disappear, and all solutions approach to zero. This is because when the stem cell death rate is larger than the proliferation rate due to division ( $2e^{-\gamma_S t_S} > 1$ ), the stem cell population (and, of course, other cell populations) will eventually decrease to zero. In fact, this is just the state of extinction.

Periods of the oscillatory solutions are shown in Figs. 2d–f. The results show obvious conservation of periods of about 20 days for the oscillatory solution with different values of parameters. This is consistent with observations from CN patients that different patients show almost the same period of oscillations (Haurie et al., 1999a). From Figs. 2d–f in addition to the 20 day periodic oscillations, there are oscillatory solutions with longer periods. Long period oscillations are also observed in CN patients (Haurie et al., 1998). From the simulations, we see that unlike the typical 20 day periods, the longer periods depend on the bifurcation parameters. Two oscillatory solutions with short and long periods, respectively, are shown in Fig. 3.

To identify the oscillatory solutions corresponding to the oscillations in CN, we calculated the severity index for each oscillatory solution. The results are shown in Figs. 2g–i. Shaded regions show the parameter values at which there are oscillatory solutions with a period of about 20 days and a severity index of about 0.20, in accordance with the observed situation in CN patients.

These simulation results suggest two possible mechanisms that may lead to oscillations in CN patients:

**Mechanism1** Decreasing the neutrophil precursor proliferation rate. In particular, when  $2.75 < \eta_N < 3.10$ , 3–15% less than the normal value, and other parameters are as in Table 2.

**Mechanism2** Increasing the HSC apoptosis rate. In particular, when  $0.10 < \gamma_S < 0.14$ , 40–100% larger than the normal value, and other parameters are as in Table 2.

The above results are consistent with previous studies (Bernard et al., 2003), and give more explicit parameter value regions for CN patients. The numerical simulations show that both mechanisms are capable of producing concomitant oscillations in erythrocyte and platelet populations, and both with the same period as neutrophils.

We note that when  $0.1 < \theta_1 < 0.35$ , there are oscillatory solutions showing a severity index close to that observed clinically. However, we cannot conclude that decreasing  $\theta_1$  is a mechanism for the oscillations in CN. The reason is that the steady state is stable in this case, and therefore decreasing  $\theta_1$  alone is not able to induce the oscillation.

### 3.2. Effect of the initial functions

In the previous section, we have shown that the hematopoietic regulatory system may display multistability, co-existence of a stable steady state and an oscillatory state, when system parameters take normal values (the healthy state). As a result, CN that is caused by changes in system parameters may not recover to the healthy state even if the parameters are taken back to their normal values by therapy, for example through G-CSF treatment. For patients with G-CSF treatment, their neutrophil count could either be stabilized or show larger amplitude oscillations (Hammond et al., 1989; Haurie et al., 1999b). Modeling simulation has also shown that the outcome of a treatment depends on the temporal protocol as well as the starting time (Foley and Mackey, 2006; Colijn et al., 2007). Mathematically, the reason for this diverse outcome is that there are delays in the hematopoietic model, and therefore the historical state prior to the treatment is important for the ultimate effect. Here, we study the effect of the initial functions on the dynamical behavior. Next, we will propose a hybrid treatment method that capable of abolishing the oscillation in CN patients.

To study the effect of initial functions, we set the system parameters at their default values as given in Table 2, and vary the initial functions in the simulation. Each solution converges to

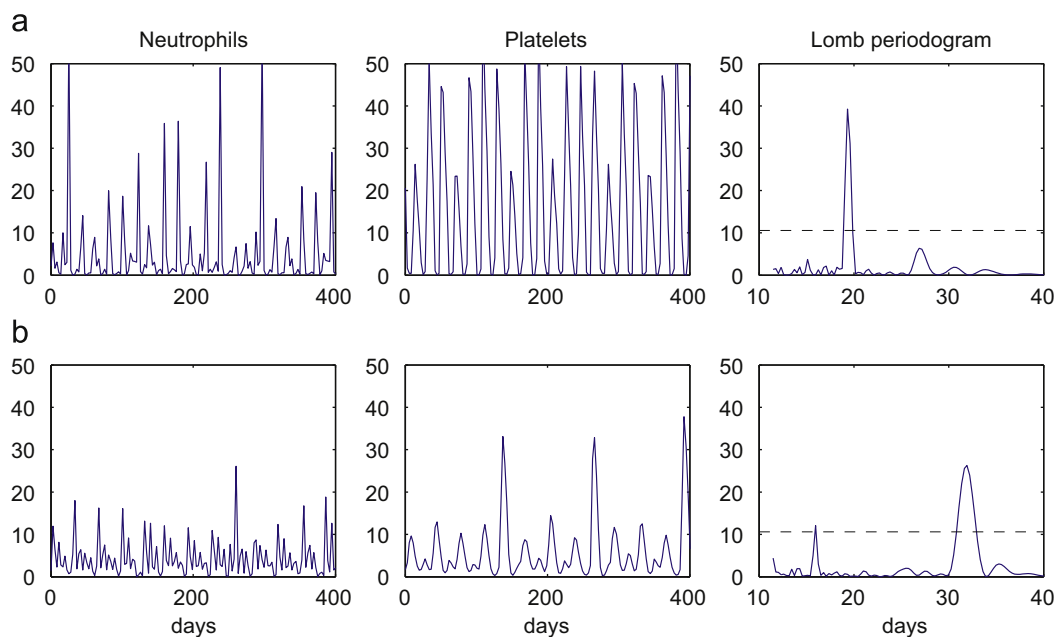


**Fig. 3.** Two numerical solutions with (a) short (19 days) and (b) long (32 days) periods, respectively. The Lomb periodograms of the neutrophils are also shown. Dashed lines show the 0.01 significance level. In both solutions,  $\eta_N = 2.78 \text{ days}^{-1}$ . Neutrophils are in units of  $10^8 \text{ cells/kg}$ , while platelets are in units of  $10^{10} \text{ cells/kg}$ .

either a stable steady state or to an oscillatory solution. From the model Eq. (9), the initial functions depend on the initial population distributions  $g_i(a)$ ,  $i=(S, N, R, P)$ , which are infinite dimensional. To illustrate the basins of attraction of the stable states in a one dimensional diagram, we characterize the initial cell populations by daily relative displacements  $\Psi_X(X=N,R,P)$  as follows. For each of the circulating cell lines, the relative displacement is defined by its distance from the steady state over the lag time and normalized by the corresponding value of the steady state:

$$\Psi_X = \frac{1}{\tau_X} \int_0^{\tau_X} \left| \frac{X(t) - X_*}{X_*} \right| dt \quad (X=N,R,P). \quad (13)$$

Here  $\tau_N = \tau_{NM}, \tau_R = \tau_{Rsum}$  and  $\tau_P = \tau_{Psum}$ . Figs. 4a–c show the dependence of  $Q_{max}$  and  $Q_{min}$  for each solution with  $\Psi_X(X=N,R,P)$ , respectively.

We consider the relationship with  $\Psi_P$  for illustration. There are two critical values ( $\Psi_1 = 0.0304$  and  $\Psi_2 = 0.8633$ ). In our simulations, all solutions with  $\Psi_P < \Psi_1$  converge to the stable steady state, and all solutions with  $\Psi_P > \Psi_2$  converge to an oscillatory state. When  $\Psi_1 < \Psi_P < \Psi_2$ , the solution converges to either the steady state or an oscillatory state, depending on the initial populations. Similar results hold for  $\Psi_N$  and  $\Psi_R$ . These results indicate that in CN therapy, simply resetting the parameters of a patient does not ensure the elimination of oscillations because the relative displacements prior the treatment are usually not small values.

Because of the multistability when system parameters take values characteristic of a healthy state, it is interesting to know how stable the steady state is to prevent a healthy person from switching to an oscillatory blood cell count. From Fig. 4b, blood cell counts of a healthy person can switch to oscillatory state if there are abnormal fluctuations such that the relative displacement  $\Psi_R > 0.28$ , i.e., about 28% away from the normal level. When  $\Psi_R < 0.28$ , Fig. 4d shows the relative displacements for the other two cell lines ( $\Psi_N, \Psi_P$ ) so that a solution remains at steady state (green points) or switches to an oscillatory state (blue points). Fig. 4e plots the probability of having an oscillatory solution as a

function of  $\Psi_N + \Psi_P$  according to the simulations, in which the dashed line shows the 50% probability level. We can see that even when  $\Psi_N + \Psi_P$  is as large as 0.8, 50% of the simulating solutions can still converge to the stable steady state. These results reveal that small fluctuation in the cell populations is not likely, if not impossible, to switch the steady state to an oscillatory state.

### 3.3. Hybrid treatment to abolish the oscillation

In Fig. 4, we note that all solutions with  $\Psi_P < 0.03$  converge to the steady state, irrespective of other cell lines. This suggests that if we could temporarily control the circulating cell populations at their normal values for some days, say 16 days ( $\approx \tau_{Psum}$ ), it would be able to abolish the oscillations. To test this idea, we propose a new therapy method for CN patients that combines G-CSF treatment and temporal blood transfusion/hemospasia. The G-CSF administration tends to force the system parameters to their default values at healthy state, and blood transfusion/hemospasia is intended to maintain the circulating cell populations at their normal levels. The effects of this hybrid treatment are studied numerically.

We started from an oscillatory state (neutrophil counts shown in lower panel in Fig. 5a), and simulated  $10^4$  sample cases, each with a randomly selected starting day of treatment and duration (in days) of blood transfusion/hemospasia. The results are shown in Fig. 5. Fig. 5a shows the cases in which the oscillations are abolished after treatment. The results suggest that if we apply transfusion/hemospasia for long enough ( $\geq 16$  days), the oscillations can be abolished no matter when we start the treatment. If the transfusion/hemospasia is shorter than 16 days, however, the effect depends on the day when the treatment is started. In isolated situations, the G-CSF treatment alone is able to abolish the oscillation (arrows in Fig. 5a). Two sample cases are shown in Fig. 5b with stabilization and oscillatory outcomes after treatment, respectively.

The disadvantage of the above protocol is the 16 days of continuous transfusion/hemospasia, which is clinically not

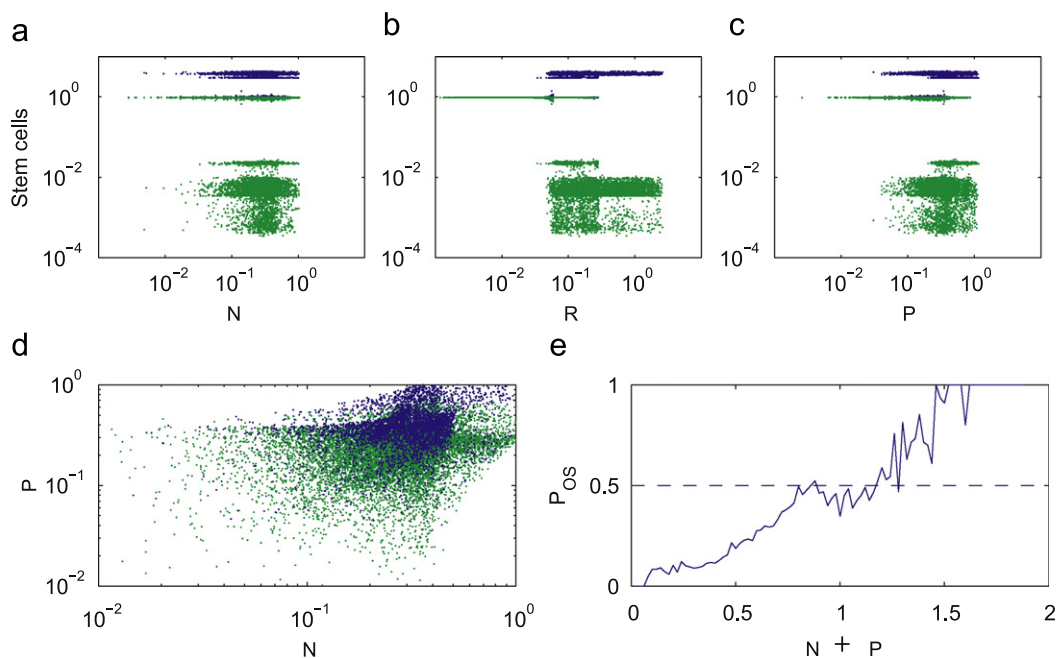


**Fig. 4.** Effect of the initial functions. (a)–(c) The maximum (blue circle) and minimum (green plus) values of stem cell counts (in units of  $10^6$  cells/kg) vs. the relative displacement between the initial function and the corresponding steady state (see the text for details) for each of the cell lines: (a) neutrophils, (b) leukocytes, and (c) platelets. (d) Basins of the stable steady state (green points) and the oscillatory solutions (blue points) represented by the displacements  $\Psi_P$  and  $\Psi_N$  (under the condition  $\Psi_R < 0.28$ ). (e) Probability to obtain oscillatory solutions ( $P_{05}$ ) as a function of  $\Psi_N + \Psi_P$  according to simulations (under the condition  $\Psi_R < 0.28$ ). Dashed line shows the 50% probability. (For interpretation of the references to colour in this figure legend, the reader is referred to the web version of this article.)

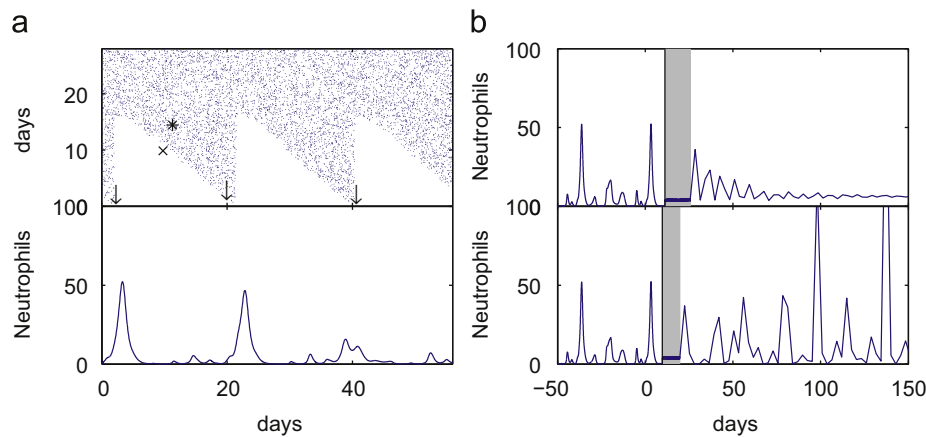


**Fig. 5.** Simulation results of the effects of the hybrid treatment combining G-CSF and blood transfusion/hemospasia. (a) Lower panel shows neutrophil counts (in units of  $10^8$  cells/kg) of an untreated case. Blue dots in the upper panel shows the cases such that oscillations are abolished after treatment. Here, the X-axis is the starting date of therapy (the same day as shown in the lower panel), and Y-axis is the number of days of transfusion/hemospasia. Arrows show that G-CSF treatment alone, starting at a proper time, is able to abolish the oscillation. (b) Two simulation results that either converge to stable steady state (upper panel) or a stable oscillatory state (lower panel) after treatment. The parameters (starting point and duration of transfusion/hemospasia) are marked by "\*" (upper panel) and "x" (lower panel) in (a), respectively. Bold vertical line shows the day of starting G-CSF administration, and shadowed areas show the days of transfusion/hemospasia. In the temporal plots, the cell counts of neutrophils (in units of  $10^8$  cells/kg) are shown. In the simulation, the starting point and duration of transfusion/hemospasia are chosen randomly from 0–8 and 0–4 weeks, respectively. We set  $\eta_N = 2.78$  for the untreated case, and  $\eta_N = 3.2$  to mimic the effect of G-CSF treatment (increased neutrophil proliferation rate). During the days of blood transfusion/hemospasia, the circulating cell populations are forced to their steady state levels (within errors of  $\pm 20\%$ ). (For interpretation of the references to colour in this figure legend, the reader is referred to the web version of this article.)

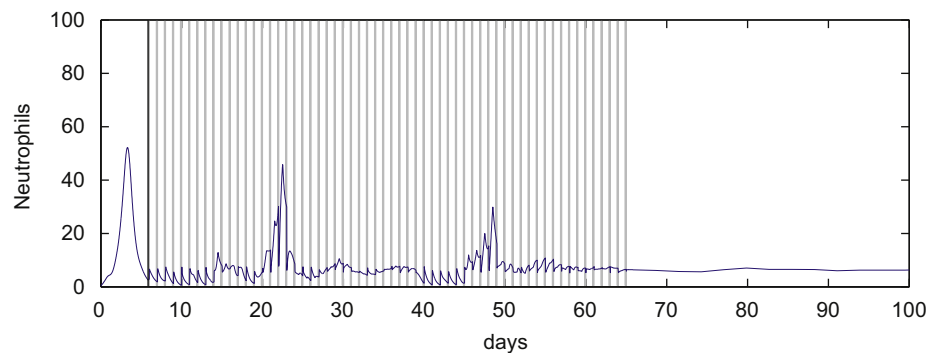


**Fig. 6.** Simulation result of neutrophil (in units of  $10^8$  cell/kg) temporal dynamics after G-CSF administration and discontinuous transfusion/hemospasia. Bold vertical line shows the day of starting G-CSF administration, and shadowed regions show the time of transfusion/hemospasia.

realistic. Here, we study the alternative option of performing transfusion/hemospasia 4 h every day. Simulations show that the G-CSF treatment together with temporal (60 days) discontinuous transfusion/hemospasia can also abolish the oscillation (Fig. 6). In this paper, we will not extend our discussion on how to design a more realistic treatment protocols, and leave it to further studies.

#### 4. Conclusions

We have studied an age-structured model of the hematopoietic system from which the model of delay differential equations and corresponding initial conditions were obtained. The models were studied numerically to investigate all possible stable solutions for given parameters. Our simulations show that the initial conditions of the delay differential equations are important because of the multistability, stable steady state and oscillatory state coexist when system parameters take values characteristic of a healthy human.

From our simulations, we have obtained oscillatory solutions that share similar dynamical features as in CN patients: (1) conservation of oscillation periods (about 20 days) for different patients, which is shown by the independent of periods with  $\eta_N$  and  $\gamma_S$ , and (2) the

neutrophil counts falling to extremely low levels for 3–5 days every three weeks. These oscillatory solutions can be induced by either decreasing the neutrophil precursor proliferation rate  $\eta_N$  (by increasing the apoptosis rate of precursor cells), or increasing the HSC apoptosis rate  $\gamma_S$ . The healthy state can be destabilized by either decreasing  $\eta_N$  or increasing  $\gamma_S$ , and converges to an oscillatory solution.

A traditional way to treat CN is trying to revert the system parameters to normal. For example, through G-CSF administration that decreases apoptosis in neutrophil precursors, and therefore leads to an increase in  $\eta_N$ . Nevertheless, such treatments may not be effective even if we can restore the system parameters to their healthy state values because of the multistability, by which the oscillatory state remains stable at the system with healthy state values. As seen clinically, it is very unusual to abolish the oscillations in CN by G-CSF administration. Thus, in therapy, we may need not only a traditional treatment that tends to recover the patient's physical symptoms, such that the healthy state is stabilized, but also an adjuvant therapy that can switch the patient from the state of oscillation to stable cell counts. The former relates to the bifurcation of the model equations and only depends on system parameters, while the latter is associated with transition of the system state from the basin of oscillatory state to that of the steady



state, and depends on the historical dynamics prior to the starting of treatment.

In this paper, we have numerically investigated the relation between a solution’s long term behavior and its initial functions. In our simulations, we found that with default value (healthy state) parameters, all solutions with small value of relative displacement for platelets for days in accordance with  $\tau_{psum}$  can always converge to the steady state, irrespective of other cell lines. This suggests a way to switch an oscillatory solution to a locally stable steady state: maintain the circulating cell populations at their normal level for some days, say 16 days. Accordingly, we propose a hybrid therapy method for CN patients that combines long term G-CSF treatment and temporarily blood transfusion/hemospasia. G-CSF tends to reset the system parameters to their normal values, and transfusion/hemospasia will keep the circulating cell populations at their normal levels. Our simulations have shown that the oscillations can be abolished if we apply transfusion/hemospasia for a long enough duration of time, say more than 16 days. Since it is not realistic to perform 16 days of continuous transfusion/hemospasia, we also studied the possibility of an alternative method with transfusion/hemospasia 4 h every day, for 60 days. Further studies are surely needed to design more realistic protocols of such hybrid treatments.

**Acknowledgements**

MCM would like to acknowledge the generous support of the Natural Sciences and Engineering Research Council (Canada), the Mathematics of Information Technology and Complex Systems (Canada) and the Alexander von Humboldt Stiftung (Germany). JL is supported by the National Natural Science Foundation of China (NSFC 10971113), and the Scientific Research Foundation for the Returned Overseas Chinese Scholars, State Education Ministry (China).

**Appendix A. Formulation for the functions  $F_i(t) (i = Q, N, R, P)$**

We refer to the general age-structured model of Fig. 7 to derive  $F_i(t) (i = Q, N, R, P)$  in the equation for the initial functions. Let  $u(t, a)$  be the circulating cell population at time  $t$  with age  $a$ . The age  $a=0$  indicates the time of differentiating from the stem cell compartment. The population dynamics are modeled by

$$\begin{cases} \frac{\partial u}{\partial t} + \frac{\partial u}{\partial a} = \eta u, & (t > 0, 0 < a < \tau_0) \\ \frac{\partial u}{\partial t} + \frac{\partial u}{\partial a} = -\gamma u, & (t > 0, \tau_0 < a < \tau) \\ u(t, 0) = f(U(t), t), & (t > 0, a = 0) \\ u(0, a) = g(a), & (t = 0, 0 \leq a \leq \tau) \end{cases} \quad (14)$$

where  $\tau_0$  is the maturation time, and  $\tau_1$  is the time to senescence,  $\tau = \tau_0 + \tau_1$ ,  $\eta$  is the proliferation rate,  $\gamma$  is the death rate,  $g(a)$  is the

initial population distribution,  $f(U(t), t)$  is the differentiation rate, and

$$U(t) = \int_{\tau_0}^{\tau} u(t, a) da \quad (15)$$

is the total population of circulating cells. We always assume  $\tau_0 < +\infty$ .

First, we consider the case  $\tau_1 < +\infty$ . Integrating the second equation in (14), we obtain an equation for  $U(t)$ :

$$\frac{dU}{dt} = -\gamma U + u(t, \tau_0) - u(t, \tau). \quad (16)$$

The Eq. (14) can be solved by the method of characteristics. The solution is given by

$$u(t, a) = \begin{cases} g(a-t)e^{\eta t}, & (0 < t \leq a \leq \tau_0) \\ g(a-t)e^{-\gamma t}, & (0 < t + \tau_0 \leq a \leq \tau) \\ g(a-t)e^{\eta(t+\tau_0-a)-\gamma(a-\tau_0)}, & (\tau_0 \leq a \leq \tau, a-\tau_0 \leq t \leq a) \\ f(U(t-a), t-a)e^{\eta a}, & (0 < a \leq \tau_0, t \geq a) \\ f(U(t-a), t-a)e^{\eta\tau_0-\gamma(a-\tau_0)}, & (\tau_0 \leq a \leq \tau, t \geq a). \end{cases} \quad (17)$$

Thus, we have

$$u(t, \tau_0) = \begin{cases} g(\tau_0-t)e^{\eta t}, & (t \leq \tau_0) \\ f(U_{\tau_0}, t-\tau_0)e^{\eta\tau_0}, & (t \geq \tau_0) \end{cases} \quad (18)$$

and

$$u(t, \tau) = \begin{cases} g(\tau-t)e^{-\gamma t}, & (t \leq \tau_1) \\ g(\tau-t)e^{-\gamma\tau_1} + \eta(t-\tau_1), & (\tau_1 \leq t \leq \tau) \\ f(U_{\tau}, t-\tau)e^{-\gamma\tau_1}, & (t \geq \tau). \end{cases} \quad (19)$$

Here  $U_{\tau_0} = U(t-\tau_0)$ ,  $U_{\tau} = U(t-\tau)$ .

Applying (18) and (19) to (16), we have the following delay differential equation for  $U(t)$  when  $t > \tau$ ,

$$\frac{dU}{dt} = -\gamma U + e^{\eta\tau_0}f(U_{\tau_0}, t-\tau_0) - e^{\eta\tau_0-\gamma\tau_1}f(U_{\tau}, t-\tau), \quad (t > \tau). \quad (20)$$

When  $t \leq \tau$  and  $\tau_0 < \tau_1$ ,

$$\frac{dU}{dt} = -\gamma U + \begin{cases} g(\tau_0-t)e^{\eta t} - g(\tau-t)e^{-\gamma t}, & (t \leq \tau_0) \\ e^{\eta\tau_0}f(U_{\tau_0}, t-\tau_0) - g(\tau-t)e^{-\gamma t}, & (\tau_0 \leq t \leq \tau_1) \\ e^{\eta\tau_0}f(U_{\tau_0}, t-\tau_0) - g(\tau-t)e^{\eta(t-\tau_1)-\gamma\tau_1}, & (\tau_1 \leq t < \tau) \end{cases} \quad (21)$$

When  $t \leq \tau$  and  $\tau_1 < \tau_0$ ,

$$\frac{dU}{dt} = -\gamma U + \begin{cases} g(\tau_0-t)e^{\eta t} - g(\tau-t)e^{-\gamma t}, & (t \leq \tau_1) \\ g(\tau_0-t)e^{\eta t} - g(\tau-t)e^{\eta(t-\tau_1)-\gamma\tau_1}, & (\tau_1 \leq t \leq \tau_0) \\ e^{\eta\tau_0}f(U_{\tau_0}, t-\tau_0) - g(\tau-t)e^{\eta(t-\tau_1)-\gamma\tau_1}, & (\tau_0 \leq t \leq \tau). \end{cases} \quad (22)$$

Thus, the full equation for  $t \geq 0$  is obtained through the initial population distribution  $g(a)$  by combining (21) or (22) with (20). The initial condition is given by  $U(0) = \int_{\tau_0}^{\tau} g(a) da$ .

If  $\tau_1 = \infty$ , the Eqs. (20)–(22) become

$$\frac{dU}{dt} = -\gamma U + \begin{cases} g(\tau_0-t)e^{\eta t}, & (t \leq \tau_0) \\ e^{\eta\tau_0}f(U_{\tau_0}, t-\tau_0), & (t > \tau_0) \end{cases} \quad (23)$$

In the hematopoietic system, we have  $\tau_{RM} < \tau_{RS}$ . Thus, the functions  $F_i(t) (i = Q, N, R, P)$  can be obtained from (20)–(23).

**Appendix B. Initial cell populations in the simulation**

First, we consider the initial population in the model given in Fig. 7. In (14),  $g(a)$  measures the initial cell population distribution. With the continuity of  $u(t, a)$  at  $(0, 0)$ , we stipulate the

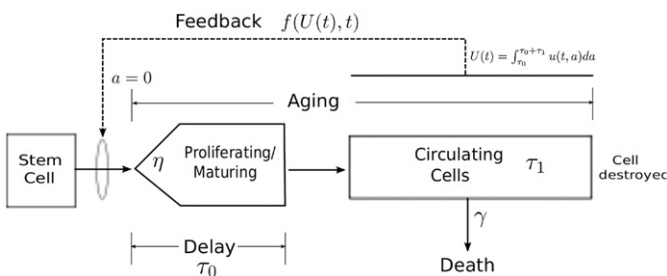


Fig. 7. Cartoon of a simple age-structured model.

condition

$$g(0) = f(U(0), 0) = f\left(\int_{\tau_0}^{\tau} g(a) da, 0\right). \tag{24}$$

Furthermore, the compatibility at (0,0) requires

$$\begin{aligned} g'(0) &= \eta g(0) - \left. \frac{\partial f}{\partial U} \right|_{(0,0)} \frac{dU(0)}{dt} - \left. \frac{\partial f}{\partial t} \right|_{(0,0)} \\ &= \eta g(0) - \left. \frac{\partial f}{\partial U} \right|_{(0,0)} (-\gamma U(0) + g(\tau_0) - g(\tau)) - \left. \frac{\partial f}{\partial t} \right|_{(0,0)}. \end{aligned} \tag{25}$$

If we select the particular initial population distribution such that the circulating cells are lost (die) at a rate  $\gamma$ , then

$$g(a) = g(\tau_0)e^{-\gamma(a-\tau_0)}, \quad (\tau_0 < a < \tau).$$

In this case, we have

$$U(0) = \int_{\tau_0}^{\tau} g(a) da = g(\tau_0)(1 - e^{-\gamma\tau})/\gamma$$

and  $g(\tau) = g(\tau_0)e^{-\gamma\tau}$ , which implies  $-\gamma U(0) + g(\tau_0) - g(\tau) = 0$ . Furthermore, when  $\partial f/\partial t|_{t=0} \equiv 0$ , the condition (25) can be reduced to

$$g'(0) = \eta g(0).$$

Thus, when  $\partial f/\partial t|_{t=0} \equiv 0$ , let  $U(0) = U_0$ ,  $g_0 = f(U_0, 0)$ , and  $g_1 = \gamma U_0/(1 - e^{-\gamma\tau})$ , it is easy to verify that the function  $g(a)$  given below satisfies the conditions (24) and (25):

$$g(a) = \begin{cases} g_0 e^{\eta a + (\ln[g_1/g_0] - \eta\tau_0)/(a/\tau_0)^2} & (0 \leq a < \tau_0) \\ g_1 e^{-\gamma(a-\tau_0)} & (\tau_0 \leq a \leq \tau) \end{cases} \tag{26}$$

In particular, we have  $g_0 = g(0)$  and  $g_1 = g(\tau_0)$ .

Now, for the hematopoietic system in the present study and for given initial values  $(Q_0, N_0, R_0, P_0)$ , we take  $(g_S(a), g_N(a), g_R(a), g_P(a))$  as follows in the simulation. First, let

$$(g_{S,0}, g_{N,0}, g_{R,0}, g_{P,0}) = (\beta(Q_0)Q_0, \kappa_N(N_0)Q_0, \kappa_R(R_0)Q_0, \kappa_P(P_0)Q_0).$$

Next, define

$$g_{S,1} = \frac{1}{2}(\beta(Q_0) + \kappa(0))Q_0,$$

$$g_{N,1} = \gamma_N N_0,$$

$$g_{R,1} = \gamma_R R_0 / (1 - e^{-\gamma_R \tau_{RS}}),$$

$$g_{P,1} = \gamma_P P_0 / (1 - e^{-\gamma_P \tau_{PS}}).$$

Now, the initial populations are

$$g_S(a) = g_{S,0} e^{-\gamma_S a + (\ln[g_{S,1}/g_{S,0}] + \gamma_S \tau_S)(a/\tau_S)^2}, \quad (0 \leq a \leq \tau_S) \tag{27}$$

$$g_N(a) = \begin{cases} g_{N,0} e^{\eta_N a + (\ln[g_{N,1}/g_{N,0}] - \eta_N \tau_{NM})(a/\tau_{NM})^2} & (0 \leq a \leq \tau_{NM}) \\ g_{N,1} e^{-\gamma_N(a-\tau_{NM})} & (a > \tau_{NM}) \end{cases} \tag{28}$$

$$g_R(a) = \begin{cases} g_{R,0} e^{\eta_R a + (\ln[g_{R,1}/g_{R,0}] - \eta_R \tau_{RM})(a/\tau_{RM})^2} & (0 \leq a \leq \tau_{RM}) \\ g_{R,1} e^{-\gamma_R(a-\tau_{RM})} & (\tau_{RM} < a \leq \tau_{Rsum}) \end{cases} \tag{29}$$

$$g_P(a) = \begin{cases} g_{P,0} e^{\eta_P a + (\ln[g_{P,1}/g_{P,0}] - \eta_P \tau_{PM})(a/\tau_{PM})^2} & (0 \leq a \leq \tau_{PM}) \\ g_{P,1} e^{-\gamma_P(a-\tau_{PM})} & (\tau_{PM} < a \leq \tau_{Psum}). \end{cases} \tag{30}$$

In the simulation, we take  $(Q_0, N_0, R_0, P_0)$  randomly, and define the initial populations  $(g_S(a), g_N(a), g_R(a), g_P(a))$  according to the above process. Next, the model Eqs. (9) can be solved numerically.

**References**

Abkowitz, J.L., Holly, R.D., Hammond, W.P., 1988. Cyclic hematopoiesis in dogs: studies of erythroid burst forming cells confirm and early stem cell defect. *Exp. Hematol.* 16, 941–945.

Adamson, J.W., 1999. The relationship of erythropoietin and iron metabolism to red blood cell production in humans. *Semin. Oncol.* 2, 9–15.

Apostu, R., Mackey, M.C., 2008. Understanding cyclical thrombocytopenia: a mathematical modeling approach. *J. Theor. Biol.* 251, 297–316.

Bélair, J., Mackey, M.C., 1987. A model for the regulation of mammalian platelet. *Ann. NY Acad. Sci.* 504, 280–282.

Bélair, J., Mackey, M.C., Mahaffy, J.M., 1995. Age-structured and two-delay models for erythropoiesis. *Math. Biosci.* 128, 317–346.

Bernard, S., Bélair, J., Mackey, M.C., 2003. Oscillations in cyclical neutropenia: new evidence based on mathematical modeling. *J. Theor. Biol.* 223, 283–298.

Beutler, E., Lichtman, M.A., Coller, B.S., Kipps, T., 1995. *Williams Hematology*. McGraw-Hill, New York.

Colijn, C., Mackey, M.C., 2005a. A mathematical model of hematopoiesis: I. Periodic chronic myelogenous leukemia. *J. Theor. Biol.* 237, 117–132.

Colijn, C., Mackey, M.C., 2005b. A mathematical model of hematopoiesis: II. Cyclical neutropenia. *J. Theor. Biol.* 237, 133–146.

Colijn, C., Mackey, M.C., 2007. Bifurcation and bistability in a model of hematopoietic regulation. *SIAM J. Appl. Dyn. Syst.* 6, 378–394.

Colijn, C., Foley, C., Mackey, M.C., 2007. G-CSF treatment of canine cyclical neutropenia: a comprehensive mathematical model. *Exp. Hematol.* 37, 898–907.

Dale, D.C., Hammond, W.P., 1988. Cyclic neutropenia: a clinical review. *Blood Rev.* 2, 178–185.

Deubelbeiss, K.A., Dancy, J.T., Harker, L.A., Finch, C.A., 1975. Neutrophil kinetics in the dog. *J. Clin. Invest.* 55, 833–839.

Dingli, D., Traulsen, A., Pacheco, J.M., 2007. Stochastic dynamics of hematopoietic tumor stem cells. *Cell Cycle* 6, 461–466.

Foley, C., Mackey, M.C., 2006. Cost-effective G-CSF therapy strategies for cyclical neutropenia: mathematical modelling based hypotheses. *J. Theor. Biol.* 238, 754–763.

Foley, C., Mackey, M.C., 2009. Dynamic hematological disease: a review. *J. Math. Biol.* 58, 285–322.

Foo, J., Drummond, M.W., Clarkson, B., Holyoake, T., Michor, F., 2009. Eradication of chronic myeloid leukemia stem cells: a novel mathematical model predicts no therapeutic benefit of adding G-CSF to imatinib. *PLoS Comput. Biol.* 5, e1000503.

Fortin, P., Mackey, M.C., 1999. Periodic chronic myelogenous leukaemia: spectral analysis of blood cell counts and aetiological implications. *Br. J. Haematol.* 104, 336–345.

Gill, M., Ockelford, P., Morris, A., Bierre, T., Kyle, C. 2000. *Diagnostic Handbook—The interpretation of Laboratory Tests*. Technical Report, Diggnostic Medlab, Auckland.

Guery, D.H., Dale, D.C., Omine, M., Perry, S., Wolff, S.M., 1973. Period hematopoiesis in human cyclic neutropenia. *J. Clin. Invest.* 52, 3220–3230.

Hammond, W.P., Price, T.H., Souza, L.M., Dale, D.C., 1989. Treatment of cyclic neutropenia with granulocyte colony stimulating factor. *N. Eng. J. Med.* 320, 1306–1311.

Haurie, C., Mackey, M.C., Dale, D.C., 1998. Cyclical neutropenia and other periodic hematological diseases: a review of mechanisms and mathematical models. *Blood* 92, 2629–2640.

Haurie, C., Person, R., Dale, D.C., Mackey, M.C., 1999a. Hematopoietic dynamics in grey collies. *Exp. Hematol.* 27, 1139–1148.

Haurie, C., Dale, D.C., Mackey, M.C., 1999b. Occurrence of periodic oscillations in the differential blood counts of congenital, idiopathic, and cyclical neutropenic patient before and during treatment with G-CSF. *Exp. Hematol.* 27, 401–409.

Haurie, C., Dale, D.C., Rudnicki, R., Mackey, M.C., 2000. Modeling complex neutrophil dynamics in the grey collie. *J. Theor. Biol.* 24, 505–519.

Hearn, T., Haurie, C., Mackey, M.C., 1998. Cyclical neutropenia and the peripheral control of white blood cell production. *J. Theor. Biol.* 192, 167–181.

Koury, M., 1992. Programmed cell death (apoptosis) in hematopoiesis. *Exp. Hematol.* 20, 391–394.

Lei, J., Mackey, M.C., 2007. Stochastic differential delay equation, moment stability, and application to hematopoietic stem cell regulation system. *SIAM J. Appl. Math.* 67, 387–407.

Lomb, N.R., 1976. Least-squares frequency analysis of unequally spaced data. *Astrophys. Space Sci.* 39, 447.

Lund, J.E., Padgett, G.A., Ott, R.L., 1967. Cyclic neutropenia in grey collie dogs. *Blood* 29, 452–461.

Mackey, M.C., 1978. Unified hypothesis for the origin of aplastic anemia and periodic haematopoiesis. *Blood* 51, 941–956.

Mackey, M.C., 1979. Periodic auto-immune hemolytic anemia: an induced dynamical disease. *Bull. Math. Biol.* 41, 829–834.

Mackey, M.C., 1996. Mathematical models of hematopoietic cell replication and control. In: Othmer, H., Adler, F., Lewis, M., Dallon, J. (Eds.), *The Art of Mathematical Modeling: Case Studies in Ecology, Physiology and Biofluids*. Prentice-Hall, pp. 149–178.

Mahaffy, J.M., Bélair, J., Mackey, M.C., 1998. Hematopoietic model with moving boundary condition and state dependent delay: application in erythropoiesis. *J. Theor. Biol.* 190, 135–146.

Marciniak-Czochra, A., Stiehl, T., Ho, A.D., Jäger, W., Wagner, W., 2009. Modeling of asymmetric cell division in hematopoietic stem cells—regulation of self-renewal is essential for efficient repopulation. *Stem Cells and Dev.* 18, 377–385.

Migliaccio, A.R., Migliaccio, G., Dale, D.C., Hammond, W.P., 1990. Hematopoietic progenitors in cyclic neutropenia: effect of granulocyte colony stimulating factor in vivo. *Blood* 75, 1951–1959.

Milton, J.G., Mackey, M.C., 1989. Periodic haematological diseases: mystical entities of dynamical disorders? *J. R. Coll. Phys.* 23, 236–241.

Novak, J.P., Necas, E., 1994. Proliferation differentiation pathways of murine haematopoiesis: correlation of lineage fluxes. *Cell. Prolif.* 27, 597–633.

- Ostby, I., Kvalheim, G., Rusten, L.S., Grottum, P., 2004. Mathematical modeling of granulocyte reconstitution after high-dose chemotherapy with stem cell support: effect of posttransplant G-CSF treatment. *J. Theor. Biol.* 231, 69–83.
- Park, J.R., 1996. Cytokine regulation of apoptosis in hematopoietic precursor cells. *Curr. Opin. Hematol.* 3, 191–196.
- Pavord, S., Sivakumaran, M., Furber, P., Michell, V., 1996. Cyclical thrombocytopenia as a rare manifestation of myelodysplastic syndrome. *Clin. Lab. Haematol.* 18, 221–223.
- Price, T.H., Chatta, G.S., Dale, D.C., 1996. Effect of recombinant granulocyte colony-stimulating factor on neutrophil kinetics in normal young and elderly humans. *Blood* 88, 335–340.
- Pujo-Menjouet, L., Mackey, M.C., 2004. Contribution to the study of periodic chronic myelogenous leukemia. *C.R. Biol.* 327, 235–244.
- Ratajczak, M.Z., Ratajczak, J., Marlicz, W., Pletcher Jr., W.C., Machalinshi, B., Moore, J., Hung, H., Gewirtz, A.M., 1997. Recombinant human thrombopoietin (TPO) stimulates erythropoiesis by inhibiting erythroid progenitor cell apoptosis. *Br. J. Haematol.* 98, 8–17.
- Roeder, I., Herberg, M., Horn, M., 2009. An “age”-structured model of hematopoietic stem cell organization with application to chronic myeloid leukemia. *Bull. Math. Biol.* 71, 602–626.
- Rubinow, S., Lebowitz, J., 1975. A mathematical model of neutrophil production and control in normal man. *J. Math. Biol.* 1, 187–225.
- Santillan, M., Mahaffy, J.M., Bélair, J., Mackey, M.C., 2000. Regulation of platelet production: the normal response to perturbation and cyclical platelet disease. *J. Theor. Biol.* 206, 585–603.
- Tanimukai, S., Kimura, T., Stakabe, H., Ohmizono, Y., Kato, T., Miyazaki, H., Yamagishi, H., Sonoda, Y., 1997. Recombinant human c-Mpl ligand (thrombopoietin) not only acts on megakaryocyte progenitors, but also on erythroid and multipotential progenitors in vitro. *Exp. Hematol.* 25, 1025–1033.
- von Schulthess, G.K., Mazer, N.A., 1982. Cyclic neutropenia (CN): a clue to the control of granulopoiesis. *Blood* 59, 27–37.
- Williams, G., Smith, C., 1993. Molecular regulation of apoptosis: genetic controls on cell death. *Cell* 74, 777–779.